Journal of Power Sources 262 (2014) 429–443

Contents lists available at ScienceDirect

Journal of Power Sources

journal homepage: www.elsevier.com/locate/jpowsour

Analytic theory for foil impedance in spiral wound cell geometries

Jan N. Reimers

388035 Mono Center Road, Mono, ON L9W6V8, Canada

HIGHLIGHTS

- Analytic solution for foil current and potentials in spiral wound cells with tabbed current collection.
- Analytic solution for cell impedance, and heat generation during discharge.
- Disentangle foil and stack impedance.
- Comparison of common and high efficiency tab arrangements.
- Worked examples for real world problems, aimed at non specialists.

ARTICLE INFO

Article history:
Received 29 November 2013
Received in revised form
6 March 2014
Accepted 8 March 2014
Available online 18 March 2014

Keywords:
Battery modeling
Foil impedance
Current collection
Analytic solution

ABSTRACT

The analytic theory for 1D foil currents and potentials in spiral wound cells with arbitrary tab configurations is derived. The theory is extended to account for state of charge gradients along the length of the foils revealing how tab geometry can affect the slope of constant current voltage curves. Analytic expressions for cell level properties are derived for common tab configurations. The quality of many tab configurations is compared. A straight forward method is described for the common, previously unsolved problem of disentangling the foil and stack contributions of a measured cell impedance. Many other examples of practical problems and solutions are presented. The analytic theory shows how to directly calculate the foil geometry factor introduced in a previous article [1]. Simple methods are presented for adding corrections for foil effects to a stack centric cell model. The analytic results provide a lot of insight and ease of use that numerical solutions cannot easily deliver.

1. Introduction

Area Specific Impedance (ASI) is a useful concept for characterizing the rate or power capability of a particular cell chemistry [2–4]. This applies for both AC and DC impedance techniques. A long-standing problem with using ASI analysis for larger cell sizes is disentangling the impedance caused by the current collection system (tabs and foils) from the stack impedance. Nelson et al. [5] were able to avoid this problem by building cells with continuous current collection (current flows in the from edge along the full length of the foils), which reduces the effective impedance of the current collection system to near zero. However it is not easy to mass produce cylindrical cells with continuous current collection. Cells with a limited number of current collector tabs placed at strategic locations along the foil length represent the vast majority of commercial cells made today. It would be very useful to find a method for subtracting the effective foil impedance from the total measured cell impedance in order to obtain an accurate estimate of the stack ASI. We will show how this can be done for any tab configuration.

To our knowledge all previous attempts to model the effect foil current and potentials have focused on using numerical methods [6–13]. In this work we will show that to a very good approximation the problem of 1D foils with randomly positioned tabs can be solved analytically. It is well known that analytic results have a lot of advantages. Most notably, they provide much deeper understanding and they are much easier to use. Others [14–17] have also made progress with analytical solutions for discharge capacity, electrolyte salt concentration and solid phase Li concentration.

The field equations for current and voltage distribution along the length of the foils (x direction) have been described previously [7]. All foils are coated on 2 sides, which means that the standard commercial spiral wound cell is actually 2 cells in parallel. In this work we use the symbol $2i_s$ for the total stack current exiting a foil layer and the current entering one stack layer will then be i_s. We will use the symbol ρ_s to represent the area specific resistivity [Ω cm^2] of one stack layer, so the resistivity of 2 layers in parallel is

E-mail addresses: janreimers@gmail.com, jan.reimers@mahyecell.ca.

http://dx.doi.org/10.1016/j.jpowsour.2014.03.018
0378-7753/

½ρ_s. A more detailed discussion appears in Ref. [7]. The field equation for a region between tabs is:

$$\nabla_x^2 \phi_s(x) = -2W(R_A + R_C) i_s(x) \tag{1}$$

where $\phi_s(x)$ is the potential across the stack, $i_s(x)$ is the current density [mA cm^{-2}] running through one layer of the stack, W is the active width, $R_A = \rho_A/W_A t_A$ is the linear resistivity [Ω cm^{-1}] of the anode foil, ρ_A is the anode foil material resistivity [Ω cm], t_A is the anode foil thickness [cm], W_A is the anode foil width [cm], with similar definitions for the cathode. Following [7], the x direction goes along the length of the spiral wound foils, y direction goes through the stack, z direction corresponds to the height of the cell or the width of the electrode foils. Eq. (1) may look like a Poisson equation, but it is not because in the source term (RHS of Eq (1)), i_s and ϕ_s are intimately related. For example if one assumes a simple Ohmic relationship as in

$$\phi_s(x) = V_o(x) - \rho_s i_s(x) \tag{2}$$

where V_o is the open circuit potential [volt] across the stack (which should not be confused with the open circuit potential of the whole cell), then one obtains

$$\left(\nabla_x^2 - \alpha^2\right)\phi_s = -\alpha^2 V_o(x) \tag{3}$$

where

$$\alpha^2 = \frac{2W(R_A + R_C)}{\rho_s}. \tag{4}$$

A differential equation with the form of Eq. (3) is commonly referred to as a modified Helmholtz equation or a screened Poisson equation.

Solving for the foil potentials in a cell design with multiple tabs is a rather complex problem. In Ref. [7] we handled this by dividing the foil length into segments, with each segment bounded by a tab or the end of the foils. Multiple instances of (3) were numerically solved, separately for each segment. The boundary conditions for each segment are related to the external boundary conditions for the cell through a system of linear equations. Solving for the segment boundary conditions is not computationally expensive, but it is difficult to program correctly. Below we show how the general problem can be handled with just one segment, which should be easier to understand and program.

We have attempted to make this article somewhat comprehensive and provide a number of expressions for the various cell properties in tables and appendices. Casual readers can jump to the results section to see how tab configurations affect cell impedance, or to the Worked Examples section for step by step instructions on how to use this technology to solve real world problems.

2. Single segment theory

2.1. Reduced units

Before proceeding it will be useful to use dimensionless units in the x direction,

$$X = \frac{x}{L}$$

where L is the total active length in the x direction. We will also define $\lambda = \alpha L$. The reader is reminded that $(\partial^2/\partial x^2) = \nabla_x^2 = (1/L^2)(\partial^2/\partial X^2) = (1/L^2)\nabla_X^2$.

2.2. Derivation of field equations

The divergence of the foil current must account for current flow through the stack and current flow from the tabs. The stack portion is smooth, and the tabs portion can be approximated with Dirac delta functions [18], $\delta(x)$. This is approximate because the tabs and the welds between the tabs and foils will have finite width, but this width is very narrow in comparison to the length of the foils. Since the Dirac delta function is not commonly used in the electrochemistry literature it will be useful to review a few properties that will be required for understanding the developments below. One reason for developing the more complicated multisegment solution in Ref. [7] was fear of the delta function. All of the properties of the delta function required for this work are summarized in Table 1, and the delta functions and its first two integrals are plotted in Fig. 1. With Table 1 under our belt, fear of the delta function becomes unwarranted.

For a cell with an arbitrary number of tabs, the foil current divergences are

$$\nabla_X I_A(X) = -2LWi_s(X) + I\sum_{j\in A}^{n_A} f_j \delta(X - X_j) \tag{5}$$

$$\nabla_X I_C(X) = 2LWi_s(X) - I\sum_{j\in C}^{n_C} f_j \delta(X - X_j) \tag{6}$$

where I is the externally applied current, I_A and I_C are the currents along the anode and cathode foils, f_j is the current fraction flowing into tab j, and X_j is the location of tab j. $\sum_{j\in A}$ means that j indexes only over the anode tabs so that the anode and cathode each have a distinct set of js. For example $A = \{1,2,3,\ldots n_A\}$ and $C = \{n_A + 1, n_A + 2, n_A + 3 \ldots n_A + n_C\}$. Since these summations and their integrals will appear often we will define

$$\Sigma_C'' = \sum_{j\in C} f_j \delta(X - X_j) \tag{7}$$

$$\Sigma_A'' = \sum_{j\in A} f_j \delta(X - X_j). \tag{8}$$

$$\Sigma'' = r_A \Sigma_A'' + r_C \Sigma_C'' = \sum_j r_j f_j \delta(X - X_j) \tag{9}$$

where

$$r_j = \begin{cases} r_A = \dfrac{R_A}{R_A + R_C}, & j\in A \\ r_C = \dfrac{R_C}{R_A + R_C}, & j\in C \end{cases}$$

are the dimensionless partial foil resistances which will always satisfy $r_A + r_C = 1$. The indefinite integrals $\Sigma' = \int \Sigma'' dX$ and double integrals $\Sigma = \int \Sigma' dX$ are then easily determined from the relations in Table 1. The fractional currents obey the normalization conditions

$$\sum_{j\in C} f_j = \sum_{j\in A} f_j = 1$$

Using Ohms law we can convert (5) and (6) into expressions for foil potentials

Table 1
Properties of the Dirac delta function and the related Heaviside step function.

Property	Formula	Nomenclature
Normalization	$\int_{-\infty}^{\infty}\delta(x)dx = 1$	
Indefinite Integral	$\int\delta(x)\mathrm{d}x = H(x)$	Heaviside step function
Origin shift	$\int\delta(x-x_o)\mathrm{d}x = H(x-x_o)$	Shifted heaviside step function
Scaling	$\delta(ax) = \frac{\delta(x)}{\lvert a\rvert}$	
Step function indefinite integral	$H_j^1(x) = \int H(x-x_j)\mathrm{d}x = (x-x_j)H(x-x_j)$	Shifted ramp function
Ramp function definite integral	$\int_0^1 H_j^1(X)\mathrm{d}X = \frac{1}{2}(1-X_j)^2 \quad 0\le X_j\le 1$	

$$\nabla_X^2\phi_A = -LR_A\nabla_X I_A(X) = 2L^2WR_A i_s(X) - ILR_A\Sigma_A''$$
$$\nabla_X^2\phi_C = -LR_C\nabla_X I_C(X) = -2L^2WR_C i_s(X) + ILR_C\Sigma_C''.$$

These can then be subtracted to yield the final field equation for the stack potential

$$\nabla_X^2\phi_C - \nabla_X^2\phi_A = \nabla_X^2\phi_s = L(R_A+R_C)[-2LWi_s + I\Sigma''] \tag{10}$$

where $L(R_A + R_C)$ is the characteristic resistance [Ω] of the anode and cathode foils. Since this quantity appears almost everywhere in the analysis below we will give it a name and symbol

$$R_f = L(R_A+R_C).$$

R_f corresponds to the total impedance of the anode and cathode foils joined end to end. It is the impedance of the longest conceivable foil current path in the cell. So our final field equation for a tabbed spiral cell is

$$\nabla_X^2\phi_s = R_f[-2LWi_s + I\Sigma'']$$

For an Ohmic system we can use (2) to eliminate i_s and get the modified Helmholtz equation for the stack potential.

$$\left(\nabla_X^2 - \lambda^2\right)\phi_s = -\lambda^2 V_o(x) + IR_f\Sigma'' \tag{11}$$

where

$$\lambda^2 = L^2\alpha^2 = \frac{LWR_f}{\frac{1}{2}\rho_s} = \frac{R_f}{R_s} \tag{12}$$

We have introduced the total stack resistance $R_s = ½\rho_s/LW$ [Ω]. Our goal is to find an analytic solution for (11) and use the solution to calculate cell level properties, internal current distributions, heat generation, compare the effectiveness of different tab configurations and show how to decouple foil and stack impedances.

2.3. General solution for constant λ

We can build up solutions to (11) by solving for the Greens function with zero slope boundary conditions

$$\left(\nabla_X^2 - \lambda^2\right)\phi_G = -\delta(X-X_j), \quad \nabla_X\phi_G|_{X=0} = \nabla_X\phi_G|_{X=1} = 0 \tag{13}$$

which has the solution

$$\phi_G(X,X_j) = \frac{\cosh\lambda X_j\cosh\lambda\overline{X} + \cosh\lambda\overline{X_j}\cosh\lambda X}{2\lambda\sinh\lambda} - \frac{1}{2\lambda}\sinh(\lambda|X-X_j|) \tag{14}$$

where

$$\overline{X} = 1 - X.$$

Note that $\phi_G(X,X_j)$ is perfectly valid when tabs are at the ends of foils ($X_j = 0$ or $X_j = 1$) which means that all tabs can be treated on an equal footing, no special rules are required for terminal tabs. Fig. 2 shows a plot of $\lambda^2\phi_G(X,1/4)$ as a function of X and λ. We can see that

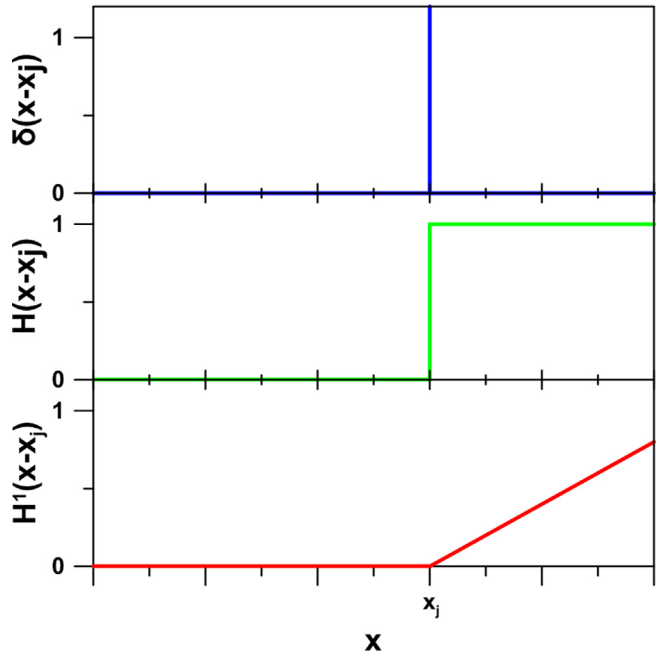

Fig. 1. Dirac delta, heaviside step and ramp functions.

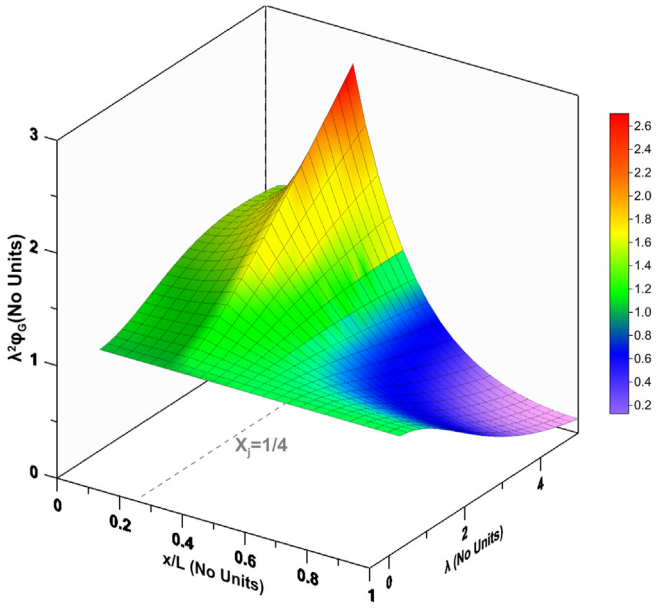

Fig. 2. Greens function, $\lambda\phi_G^2(X,X_j)$ with $X_j = 1/4$.

it is peaked at $X = X_j$ and the cusp gets sharper for larger λ. This represents the response of the stack potential for an infinitesimally narrow, unit current source at $X_j = 1/4$. For small λ the voltage response is spread out, and for large λ it is localized.

With the Greens function in hand we can build up the solution for arbitrary source functions on the RHS of Eq. (10) or (11). For example the solution to

$$\left(\nabla^2 - \lambda^2\right)\phi_V = -\lambda^2 V_o(X). \tag{15}$$

is a convolution integral

$$\phi_V(X) = \lambda^2 \int \phi_G(X,S)V_o(S)\mathrm{d}S. \tag{16}$$

The complete general solution for constant λ can now be written as follows

$$\phi_s(X) = \phi_V(X) - IR_f\Gamma(X) \tag{17}$$

where

$$\Gamma(X) = \sum_j r_j f_j \phi_G(X,X_j) \tag{18}$$

which contains all the tab geometry information.

2.4. Foil currents and potentials

We can obtain an expression for the foil currents by using (5) and (6) to eliminate the stack current in (10) which can then be integrated to give:

$$I_A(X) = \frac{\nabla_X\phi_s}{R_f} - Ir_C(\Sigma'_C - \Sigma'_A) \tag{19}$$

$$I_C(X) = \frac{-\nabla_X\phi_s}{R_f} - Ir_A(\Sigma'_C - \Sigma'_A) \tag{20}$$

Integrating once more yields explicit expressions for the foil potentials

$$\phi_A(X) = -LR_A\int I_A\mathrm{d}X = -r_A\phi_s(X) + IR_f r_A r_C(\Sigma_C - \Sigma_A) \tag{21}$$

$$\phi_C(X) = -LR_C\int I_C dX = r_C\phi_s(X) + IR_f r_A r_C(\Sigma_C - \Sigma_A) \tag{22}$$

These expressions for the foil potentials are important for two reasons, 1) they allow us to derive explicit expressions for the cell voltage and impedance under load, and 2) they are used to determine the fractional currents f_j for complex tab configurations by potential matching:

$$\phi_A(X_k) = \phi_A(X_{k+1}), \quad k\in A \tag{23}$$

$$\phi_C(X_k) = \phi_C(X_{k+1}), \quad j\in C \tag{24}$$

2.5. Cell level properties

Defining X_A as the location of any anode tab, X_C as the location of any cathode tab we can write down the external cell voltage as

$$\begin{aligned} V_{cell} &= \phi_C(X_C) - \phi_A(X_A) \\ &= r_C\phi_V(X_C) + r_A\phi_V(X_A) - IR_f(r_C\Gamma(X_C) + r_A\Gamma(X_A) \\ &\quad + r_A r_C[\Sigma(X_C) - \Sigma(X_A)]) \end{aligned} \tag{25}$$

which looks like it has the form $V_{ocv} - IR_{cell}$ with

$$R_{cell} = R_f(r_C\Gamma(X_C) + r_A\Gamma(X_A) + r_A r_C[\Sigma(X_C) - \Sigma(X_A)]). \tag{26}$$

We must be a little bit careful interpreting $r_C\phi_V(X_C) + r_A\phi_V(X_A)$ as an OCV. This quantity represents the instantaneous voltage that the cell will relax to when the current is switched off. After running the some current through the cell the state of charge will not be uniform along the length of the foils. In this case when the external current is turned off, there will still remain some internal mixing currents flowing. This will cause the external cell voltage to further relax on a longer time scale.

Up until this point we have expressed all quantities in terms of the characteristic foil resistance R_f. What happened to stack impedance in Eq. (26)? Well, it is hiding in the Γ summations, Eq. (18). It is also useful to note that because of Eq. (12), for any of the derived expressions in this article we can substitute $R_s\lambda^2$ for R_f. We prefer to use R_f because it can easily be calculated from the dimensions of the foils, whereas R_s us usually unknown.

We can also define the effective foil impedance [Ω]

$$\begin{aligned} R_{foil} &= R_{cell} - R_s \\ &= R_f\left(r_C\Gamma(X_C) + r_A\Gamma(X_A) + r_A r_C[\Sigma(X_C) - \Sigma(X_A)] - \frac{1}{\lambda^2}\right) \end{aligned} \tag{27}$$

foil fraction of the impedance as

$$f_{foil} = \frac{R_{foil}}{R_{cell}} = 1 - \frac{1}{\lambda^2(r_C\Gamma(X_C) + r_A\Gamma(X_C) + r_A r_C[\Sigma(X_C) - \Sigma(X_A)])}$$

We need to be a little careful to define the precise meaning of R_s and R_{foil}. R_s only corresponds to the total effective stack impedance if the stack current density, i_s is uniform, and this can only happen for a cell with continuous current collection. As soon as i_s becomes non-uniform the effective impedance of the stack becomes slightly larger than R_s. This excess is actually captured in the definition of R_{foil} in Eq. (27). So the term R_{foil} is a little bit misleading. Indeed R_{foil} is mostly foil impedance, but also contains a small contribution from the effective stack impedance enhancement caused by non-uniform i_s. An accurate name might be $R_{\text{enhancement over continuous current collection cell}}$. This distinction only becomes important when we disentangle the stack and foil contributions to the heat generation.

The total heat generation rate [watts] in the cell is

$$q_{cell} = q_{stack} + q_{foil} = L\int_0^1 \left(Wi_s^2(X)\rho_s + I_A^2(X)R_A + I_C^2(X)R_C\right)\mathrm{d}X$$

which includes stack, anode foil and cathode foil contributions. General expressions for the heat are rather complex and will not be presented here. Expressions for specific tab configurations will be presented below.

In Ref. [1] we described a method for modeling spiral wound cells using an empirical estimation of the effective foil impedance. In particular we approximated

$$R_{foil} = \frac{L(R_A + R_C)}{3g} \tag{28}$$

where g is the so called geometry factor which accounts for the tab geometry. Intuitive arguments were employed in order to deduce ideal values of g that were valid when i_s was assumed constant. More accurate values of g were determined by comparing with fully coupled numerical simulations. We can combine (28) and (26) to obtain an explicit expression for g

$$g = \frac{1}{3\left(r_C\Gamma(X_C) + r_A\Gamma(X_A) + r_A r_C[\Sigma(X_C) - \Sigma(X_A)] - \frac{1}{\lambda^2}\right)} \tag{29}$$

which is valid even when i_s is not constant.

2.6. Time evolution

2.6.1. Equation of motion

By re-arranging Eq. (2) as

$$\rho_s i_s(X,t) = V_o(X,t) - \phi_V(X,t) + IR_f\Gamma(X) \tag{30}$$

and taking the time derivative

$$\rho_s\frac{\partial i_s}{\partial t} = \frac{\partial V_o}{\partial t} - \lambda^2\int_0^1 \phi_G(X,S)\frac{\partial V_o}{\partial t}dS$$

we can arrive at the time evolution equation for the stack current

$$\tau(t)\frac{\partial i_s}{\partial t} = i_s(X,t) - \lambda^2\int_0^1 \phi_G(X,S)i_s(S,t)dS \tag{31}$$

where we have used

$$\frac{\partial V_o}{\partial t} = \left.\frac{\partial V_o}{\partial q}\right|_t\frac{\partial q}{\partial t} = \left.\frac{\partial V_o}{\partial q}\right|_t i_s(X,t) \tag{32}$$

and defined the time constant

$$\tau(t) = \frac{\rho_s}{\left.\frac{\partial V_o}{\partial q}\right|_t}.$$

Eq. (31) is called a Barbashin equation [19,20] with stationary kernel ϕ_G. What these equations tell us is that if the system starts out with a $V_o(X)$ that is uniform in X, and $i_s(X)$ has cusps at the tabs; then as time evolves $i_s(X)$ gets smoother and $V_o(X)$ develops peaks. For constant τ there may be hope of finding analytic solutions to (31) but in the general case we suspect that numerical integration/simulation will be required.

2.6.2. Three states of discharge

Our goal in this work is to describe a technique for comparing various tab configurations, however some tab configurations will be more efficient at the beginning of discharge and very inefficient late in the discharge and for others *vice versa*. So we need an analytically tractable way for looking at the solutions and cell properties at various states of discharge (DODs). This can be achieved by considering three special states of charge summarized in Table 2. At short times $i_s(X)$ has cusps at the tab locations and V_o is constant, somewhere midway through a discharge $i_s(X)$ becomes roughly constant and V_o had downward pointing cusps at the tab locations. Finally toward the end of a discharge $i_s(X)$ becomes inverted and is peaked between the tabs. Our definition for the late stage is

Table 2
Three special states during a constant current discharge.

Time into discharge	$i_s(X)$	$V_o(X)$	Symbol name
Early	Peaks at tabs	Constant in X	i_s^{early}
Middle	Constant in X	Dips at tabs	i_s^{middle}
Late	Dips at tabs	Dips at tabs	i_s^{late}

$$i_s^{late} = 2i_s^{middle} - i_s^{early} \tag{33}$$

Fig. 3 shows what the stack current would look like in the three states, for a tab configuration with two cathode tabs at $X = \{1,0\}$ and one anode tab at $X = \{½\}$ (configuration F4 below).

The theory for the early condition is straight forward, just assume a constant V_o, in Eqs. (15)–(17) with the result that $\phi_V = V_o$, and then carry this result through to the foil and cell properties. The theory for the middle condition contains some subtleties and is outlined in Appendix A. Since the cell voltage and impedance are both linearly related to i_s, the late state solution for these cell properties simply follows same rule as used in Eq. (33), for example

$$R_{cell}^{late} = 2R_{cell}^{middle} - R_{cell}^{early}. \tag{34}$$

Consideration of the three states of charge are only important for duty cycles that use the cell on a more or less continuous bases (constant current or closely spaced pulses). Readers who are primarily interested in pulsed applications for which the cell is allowed to relax between pulses, will only need to consider the early stage results which are applicable at any DOD provided V_o and ρ_s are defined at that DOD.

2.7. Summary

Expressions for all the relevant stack, foil and cell properties are summarized in Table 3. The general and early formulas are based on hyperbolic functions in X, whereas at the middle state the formulas are quadratic in X. This concludes the development of the general theory and solutions. In the remainder of the article we will discuss merits of specific tab configurations and a number of examples showing how the theory can be applied.

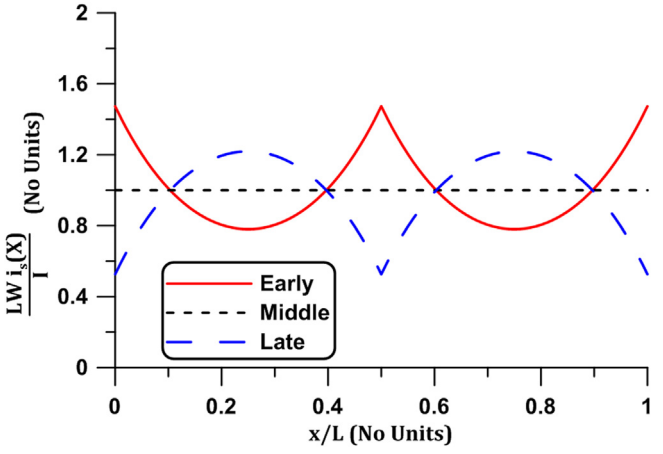

Fig. 3. Dimensionless stack current density LWi_s/I for the early, middle and late states.

Table 3
Summary of all formulas for general, early and middle state conditions.

	Symbol	General	Early $t = 0$	Middle
Conditions		None	$V_o = \text{const.}$	$i_s = \text{const}$
Stack Potential DE		$(\nabla_X^2 - \lambda^2)\phi_s = -\lambda^2 V_o + IR_f\Sigma''$	$\Leftarrow$ with const. V_o	$\nabla_X^2\phi_s = IR_f[\Sigma''(X) - 1]$
Particular DE		$(\nabla^2 - \lambda^2)\phi_V = -\lambda^2 V_o(X)$	$\Leftarrow$ with const. V_o	$\nabla^2\phi_V = -IR_f(1 - \lambda^2\Gamma(X))$
Particular Solution	$\phi_V(X)$	$\lambda^2\int\phi_G(X,S)V_o(S)\mathrm{d}S$	V_o	$IR_f\left[\frac{1}{\lambda^2} + \Sigma(X) - \frac{1}{2}X^2\right]$
Stack potential solution	$\phi_s(X)$	$\phi_V - IR_f\Gamma$	$V_o - IR_f\Gamma$	$IR_f\left[\Sigma(X) - \frac{1}{2}X^2\right] + d$
Stack current	$i_s(X)$	$\frac{V_o - \phi_V + IR_f\Gamma}{\rho_s}$	$\frac{I}{2LW}\lambda^2\Gamma$	$\frac{I}{2LW}$
Anode foil current	$I_A(X)$	$\frac{\nabla_X\phi_s}{R_f} - Ir_C(\Sigma_C' - \Sigma_A')$	$I[-\nabla_X\Gamma - r_C(\Sigma_C' - \Sigma_A')]$	$I[\Sigma_A'(X) - X]$
Cathode foil current	$I_C(X)$	$-\frac{\nabla_X\phi_s}{R_f} - Ir_A(\Sigma_C' - \Sigma_A')$	$I[\nabla_X\Gamma - r_A(\Sigma_C' - \Sigma_A')]$	$-I[\Sigma_C'(X) - X]$
Anode foil potential	$\phi_A(X)$	$-r_A\phi_s + IR_f r_A r_C(\Sigma_C - \Sigma_A)$	$\Leftarrow$	$-IR_f r_A\left[\Sigma_A(X) - \frac{1}{2}X^2\right]$
Cathode foil potential	$\phi_C(X)$	$r_C\phi_s + IR_f r_A r_C(\Sigma_C - \Sigma_A)$	$\Leftarrow$	$IR_f r_C\left[\Sigma_C(X) - \frac{1}{2}X^2\right] + d$
Cell voltage	V_{cell}	Eq. (25)	$V_o - IR_{cell}$	Eq. (A.4)
Cell impedance	R_{cell}	Eq. (26)	Eq. (26)	Eq. (A.5)

3. Results

3.1. Internal properties

It is useful to look at all the internal properties for a simple yet common tab configuration with one anode tab at $X = 0$ and one cathode tab at $X = 1$. This is tab configuration F2 in Table 5. The details of the cell are presented in Table 4. We purposely chose asymmetric foil resistances to provide understanding of this effect. The results for early, middle and late stages of the discharge are shown in Fig. 4. The following features should be noted:

- The open circuit stack potential $V_o(X)$ becomes less uniform as the discharge proceeds.
- The early stack current is peaked at the tab locations. Because the cathode foil is higher impedance we see more stack current at the cathode tab than at the anode tab.
- For the early stage, near the cathode tab the cathode foil current is suppressed and the anode foil current is enhanced. The system prefers to run as little current as possible through the higher impedance cathode foil.
- The middle stage foil currents are linear, which is just a consequence of the constant stack current.
- At the late stage the system is forced to run more foil current near the cathode tab because the active material in the stack has been depleted near the cathode tab. This means that the effective foil impedance of the cell will be enhanced at the late stage.
- The foil potentials look smooth and fairly similar, but this is deceptive. Small changes in the shape and value of the foil potentials can result in significant changes in the foil currents and stack properties.

Table 4
Sample cell design and material parameters.

Property	Units	Value
L	[cm]	80
W	[cm]	6
t	[μm]	10
ρ_A, ρ_C	[μΩ cm]	1.7, 3.1
R_A, R_C	[mΩ cm^{-1}]	0.28, 0.52
r_A, r_C	[no units]	1/3, 2/3
ρ_s	[Ω cm^2]	3.413
λ	[no units]	3
V_o	[volt]	4

This should give the reader some insight as to how tabbed cells prefer to distribute current and why. In the sections that follow we will focus on cell impedance for systems with $r_A = r_C = ½$, which is what most commercial cell designs strive to achieve. This restriction will greatly simplify the formulas presented without detracting from their practical application. This also means that for a specified tab configuration, all results are equally valid if the anode and cathode tab locations are swapped.

3.2. Cell impedance for fixed tab configurations

Table 5 shows the reduced cell impedance (R_{cell}/R_s) and geometry factor (g) expressions for a number of fixed tab configurations. For each configuration we show a drawing, list of tab locations, current fractions and the reduced impedance for the early and middle state conditions. The late stage cell impedance can easily be calculated from Eq. (34), and the corresponding geometry factor should be calculated from R_{cell}^{late} using (28). However

$$g^{late} = 2g^{middle} - g^{early} + O\left(\lambda^4\right) \tag{35}$$

is valid to second order in λ so for example for F1 $g^{late} = 1 - \lambda^2/15$ which points us towards a simple method of defining an SOC dependence for g.

Readers can simply multiply the reduced impedance expressions in Table 5 by either R_f/λ^2 or R_s in the units of choice, to get a real cell impedance. For most configurations the fractional currents were easily determined by uniqueness (only one tab) or by symmetry. For configuration F6 with three cathode tabs, the potential matching relations (24) were used to derive the unsurprising answer {1/4, ½, 1/4} for the cathode tab current fractions. Configuration F7 was purposely included as an example of what happens in a low symmetry configuration. In general the complexity of the expressions increases rapidly as the symmetry drops or the number of tabs increases.

For the early state geometry factors we have chosen to display a second order Taylor expansion rather than the full expression. For the middle state, the expressions for impedance and geometry factor are exact (not Taylor expansions). All middle state impedances are independent of the partial foil resistances. Although not evident in the table it turns out that the same is true for the early stage impedance for tab configurations F1, F3 and F5. This means that adjusting the relative thicknesses of the anode cathode foils will yield no improvement in the corresponding cell impedances for these three tab configurations.

Table 5
Fixed position tab configurations. Drawings use red for anode tabs and blue for cathode tabs.

Name	Drawing	X_j {A}{C}	f_j {A}{C}	Early		Middle	
				$\frac{R_{cell}}{R_{stack}}$	g	$\frac{R_{cell}}{R_{stack}}$	g
F1	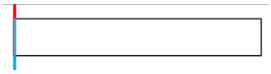	{0}{0}	{1}{1}	$\frac{\lambda\cosh\lambda}{\sinh\lambda} = \lambda\coth\lambda$	$1+\frac{\lambda^2}{15}+O(\lambda^4)$	$1+\frac{1}{3}\lambda^2$	1
F2	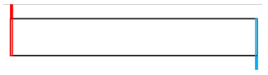	{0}{1}	{1}{1}	$\left(\frac{\lambda}{2}\right)^2+\frac{\lambda}{2\sinh\lambda}(1+\cosh\lambda)$	$1+\frac{\lambda^2}{240}+O(\lambda^4)$	$1+\frac{1}{3}\lambda^2$	1
F3		$\{\frac{1}{2}\}\{\frac{1}{2}\}$	{1}{1}	$\frac{\lambda}{2}\coth\frac{\lambda}{2}$	$4+\frac{\lambda^2}{15}+O(\lambda^4)$	$1+\frac{1}{12}\lambda^2$	4
F4		$\{\frac{1}{2}\}\{0,1\}$	$\{1\}\{\frac{1}{2},\frac{1}{2}\}$	$\left(\frac{\lambda}{4}\right)^2+\frac{\lambda}{4\sinh\frac{\lambda}{2}}\left(1+\cosh\frac{\lambda}{2}\right)$	$4+\frac{\lambda^2}{240}+O(\lambda^4)$	$1+\frac{1}{12}\lambda^2$	4
F5		$\{\frac{1}{4},\frac{3}{4}\}\{\frac{1}{4},\frac{3}{4}\}$	$\{\frac{1}{2},\frac{1}{2}\}\{\frac{1}{2},\frac{1}{2}\}$	$\frac{\lambda}{4}\coth\frac{\lambda}{4}$	$16+\frac{\lambda^2}{15}+O(\lambda^4)$	$1+\frac{1}{48}\lambda^2$	16
F6		$\{\frac{1}{4},\frac{3}{4}\}\{0,\frac{1}{2},1\}$	$\{\frac{1}{2},\frac{1}{2}\}\{\frac{1}{4},\frac{1}{2},\frac{1}{4}\}$	$\left(\frac{\lambda}{8}\right)^2+\frac{\lambda}{8\sinh\frac{\lambda}{4}}\left(1+\cosh\frac{\lambda}{4}\right)$	$16+\frac{\lambda^2}{240}+O(\lambda^4)$	$1+\frac{1}{48}\lambda^2$	16
F7	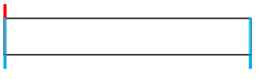	{0}{0,1}	{1}{1 − (C.1), (C.1)}	$\frac{\frac{\lambda}{2}(\lambda\cosh\lambda+\sinh\lambda)}{(\cosh\lambda-1)+\frac{\lambda}{2}\sinh\lambda}$	$\frac{8}{5}+\frac{19\lambda^2}{375}+O(\lambda^4)$	$1+\frac{5}{24}\lambda^2$	$\frac{8}{5}$

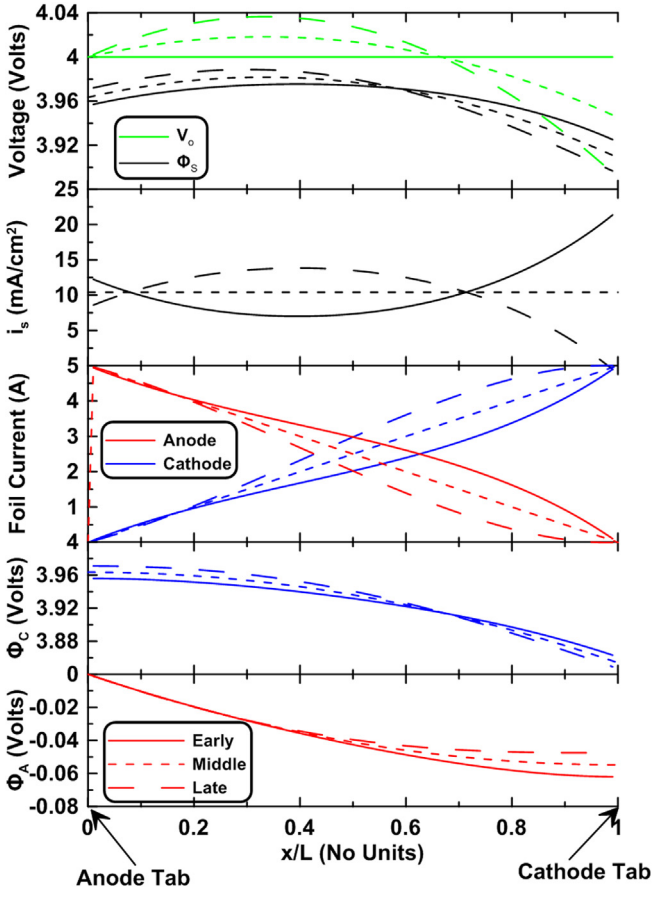

Fig. 4. Internal properties for early (solid line), middle (small dashes) and late (long dashes) stages of discharge, for the F2 tab configuration.

There are a number of interesting patterns in Table 5:

- The impedance formulas for {F1, F3, F5} make a nice sequence. And similarly for {F2, F4, F6}.
- To lowest order the geometry factors and middle stage impedance formulas make no distinction between the pairs {F1, F2}, {F3, F4} and {F5, F6}
- {F1, F3, F5} are all strongly dependent on λ (see 1/15 coefficient for g) for the early and late stages. Conversely {F2, F4, F6} are all weakly dependent on λ for the early and late stages. As a result we would expect F1 to have a steeper voltage curve than F2 but similar average voltage, and similarly for the pairs {F3, F4} and {F5, F6}.

There are a number of interesting graphical comparisons to be made. In particular F1, F2 and F3 all have two tabs. From Figs. 5 and 6 we can see that F3 is vastly superior to F1 and F2 for all states of charge and for any λ. Deciding between F1 and F2 is more subtle; F1 is superior at the early state of charge but inferior to F2 at the late stage. Hence F1 is good for pulsed applications, but F2 will have a flatter voltage curve for continuous discharge (energy) applications. We can reach the same conclusions by inspecting the Taylor expansions for g in Table 5 or inspecting the coefficients in Table 6. From Figs. 5 and 6 we can also see that the reduced foil impedance is the more sensitive value for comparing various tab configurations, for F4–F6 we only display the reduced foil impedance in Figs. 7 and 8. The general trends are now obvious, there is a first order effect for impedance {F5, F6} $\ll$ {F3, F4} $\ll$ {F1, F2} which is controlled by the first term in the Taylor expansions for g. This first order effect overwhelms any dependence on state of charge or λ. The second order effects tell which designs will have the flatter voltage curves {F2, F4, F6} and which designs are better for pulsed applications {F1, F3, F5}. In Fig. 9 we show the geometry factors for F1–F6 and also the foil impedance fractions (Fig. 10). The foil impedance and geometry factors for configurations {F2, F4, F6} look

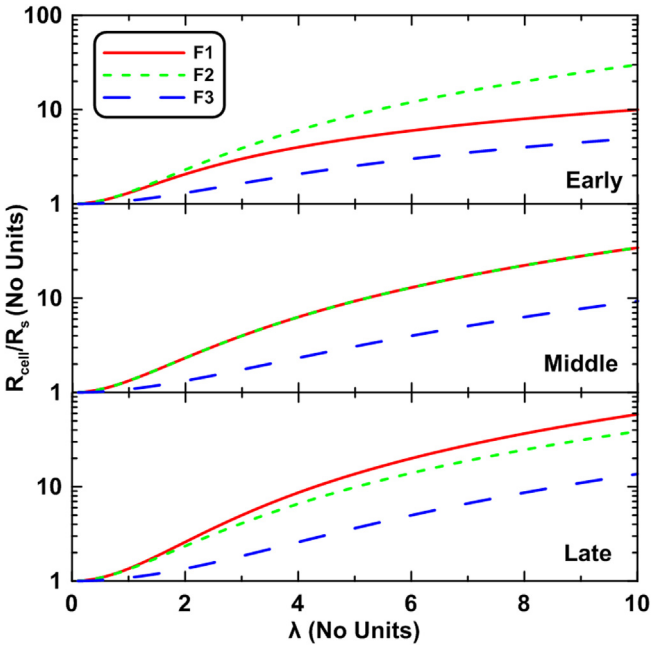

Fig. 5. Reduced cell impedance for the F1, F2 and F3 tab configurations at all three stages of discharge.

essentially flat and to a good approximation we can ignore the weak λ dependence for these cells.

In Ref. [1] we used Eq. (28) to model the foil impedance of a cell and compared the calculated voltage profile under load with a numerical simulation, using a large enough grid to give very accurate results. For a cell design with the F4 tab configuration and $\lambda \approx 8$ we found that adjusting g from the ideal value of 4 to $g = 4.2$ gave good agreement between the two calculations. For foil heating we found a slightly larger value $g = 4.3$ gave the best results. From Table 5 we see that for this design $g = 4 + \lambda^2/240$ which yields

Table 6
Taylor expansion coefficients for Eq. (37).

	A_0	A_2	A_4	B_2	B_4	Max λ
F1	$\frac{1}{3}$	$-\frac{1}{45}$	$\frac{2}{945}$	0	0	4.1
F2	$\frac{1}{3}$	$-\frac{1}{720}$	$\frac{1}{30{,}240}$	$-\frac{1}{12}$	$\frac{1}{120}$	10.3
F3	$\frac{1}{12}$	$-\frac{1}{720}$	$\frac{1}{30{,}240}$	0	0	10.3
F4	$\frac{1}{12}$	$-\frac{1}{11520}$	$\frac{1}{1{,}935{,}360}$	$-\frac{1}{192}$	$\frac{1}{7680}$	26
F5	$\frac{1}{48}$	$-\frac{1}{11{,}520}$	$\frac{1}{1{,}935{,}360}$	0	0	26
F6	$\frac{1}{48}$	$-\frac{1}{184{,}320}$	$\frac{1}{123{,}863{,}040}$	$-\frac{1}{3072}$	$\frac{1}{491{,}520}$	65
F7	$\frac{5}{24}$	$-\frac{19}{2880}$	$\frac{163}{483{,}840}$	Undefined	Undefined	6.1

$g \approx 4.26$ which is in very good agreement with the empirical adjustments carried out against the numerical simulation.

In Table 5 we chose to express the reduced cell impedance as R_{cell}/R_s for brevity reasons, however R_s is not a directly measurable quantity and it is difficult to calculate. However R_f is very easy to calculate (see Worked examples section below). Using (12) we find

$$\frac{R_{cell}}{R_f} = \frac{1}{\lambda^2}\left(\frac{R_{cell}}{R_s}\right) \tag{36}$$

which allows one to express the cell impedance in terms of R_f and the expressions in Table 5. This is only useful of we already know λ which is usually not the case. The left and side of (36) is directly measurable so we must invert (36) in order to determine λ. This is most easily achieved with a Taylor expansion

$$\frac{R_{cell}}{R_f} = \frac{1}{\lambda^2} + \frac{R_{foil}}{R_f} = \frac{1}{\lambda^2} + A_0 + (1 - 2\mathrm{DOD})\left(A_2\lambda^2 + A_4\lambda^4\right) + O\left(\lambda^6\right) \tag{37}$$

where the coefficients for all tab configurations are listed in Table 6. As is evident from (37) by simply dropping the $1/\lambda^2$ term at the beginning of the expansion we can use the same coefficients to calculate R_{foil}/R_f if desired. In Table 6 we also indicate the maximum

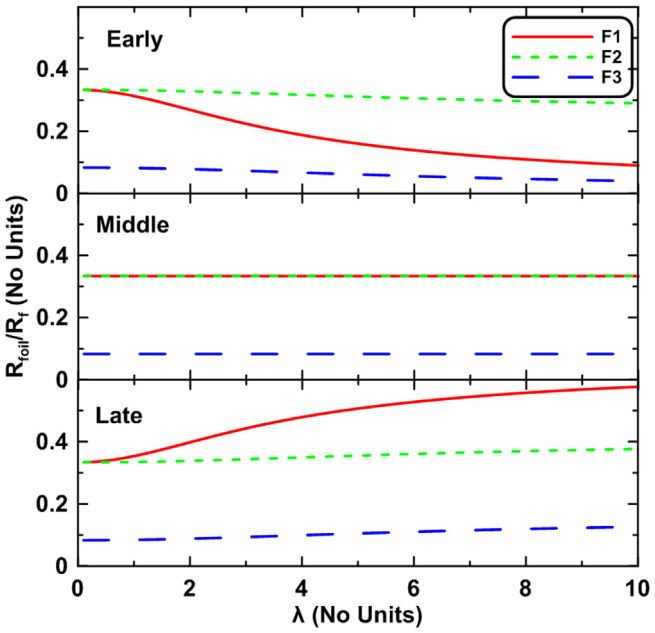

Fig. 6. Reduced foil impedance for the F1, F2 and F3 tab configurations at all three stages of discharge.

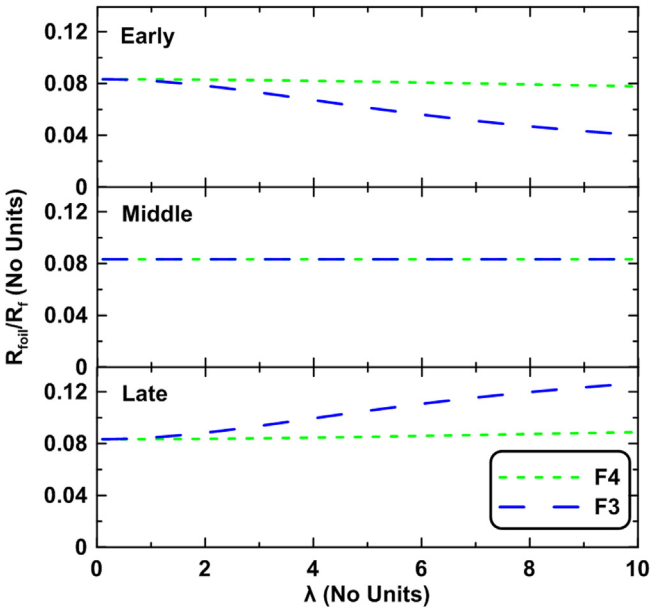

Fig. 7. Reduced foil impedance for the F3 and F4 tab configurations at all three stages of discharge.

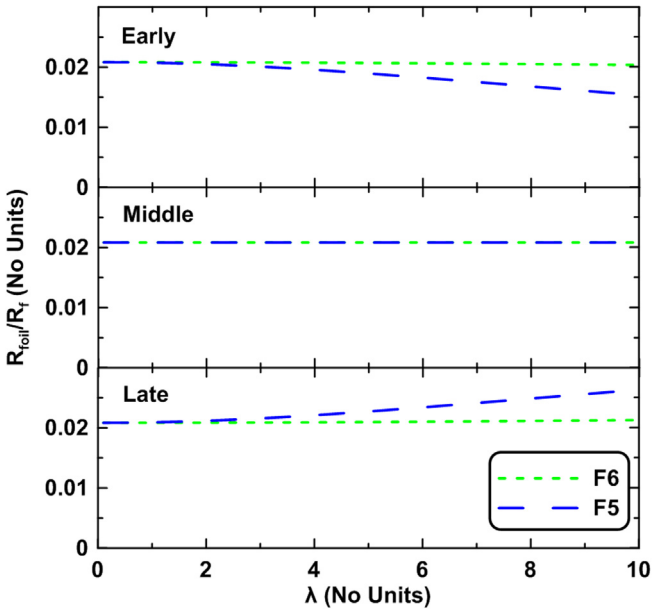

Fig. 8. Reduced foil impedance for the F5 and F6 tab configurations at all three stages of discharge.

value of λ for which the expansion (37) is accurate. Max λ is defined as the point where the sixth order term in (37) becomes of order one. Eq. (37) is the key to disentangling the foil and stack contributions to the total cell impedance. All we need is

1. A measured cell impedance (which is a routine measurement). This could be an AC, DC or pulse impedance.
2. Some basic information on the foil dimensions to calculate $R_f = L[\rho_A/(W_A t_A) + \rho_C/(W_C t_C)]$
3. The tab configuration for deciding the relevant set of expansion coefficients A_0, A_2 and A_4.

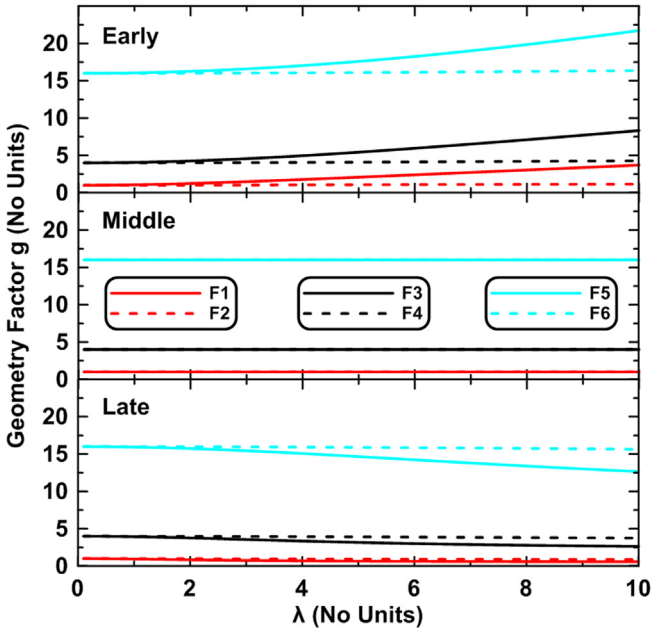

Fig. 9. Geometry factor for the F1–F6 tab configurations at all three stages of discharge.

Once λ is determined accurate estimates for all other internal and external cell properties can be calculated. See worked problem 1 below.

3.3. Cell heating for fixed tab configurations

The total heat generation for the early and middle stages of discharge can be simply calculated from I^2R_{cell}, however this is not true of the late stage total heat or for the breakdown in terms of stack and foil contributions. Expressions for the early middle and late stage foil heating rates are shown in Table 8 in reduced units q/I^2R_s. For the stack only the early stage expressions are shown, it turns out the that the late stage makes the same stack heat as the early stage as is intuitively evident from the symmetry in Fig. 3. The middle stage stack heat in reduced units is just 1.

Before discussing the results and trends it is worth understanding why in general $q_{foil} \neq I^2R_{foil}$. This is not because of approximations. As discussed above in Section 2.5 by definition R_{foil} is mostly foil impedance, but also contains a small contribution from the effective stack impedance enhancement caused by non-uniform i_s. The proper interpretation of I^2R_{foil} is: The excess heat generated by not having continuous current collection. Fig. 12 clearly shows that for the F1 tab configuration, when $\lambda > 1$ the heat calculated form I^2R_{foil} is slightly overestimated for the early stage and slightly underestimated for the late stage. The same is true for the F3 and F5 configurations. For the F2 configuration we see that this distinction is tiny, and the same is true for the F4 and F6 configurations.

Fig. 13 shows the heating breakdown for all three states of discharge and for the F1 and F2 tab configurations. As with the cell impedance, we see that for the heating of the F1 configuration, the dependence on the stage of the discharge becomes greatly amplified. F1 is not good for full discharge applications, but good for pulsed if it has time to relax between pulses. The stack heating may look small but that is only because we chose to normalize by dividing by R_s. If we had normalized with R_f we would see the stack heat diverge as $\lambda \rightarrow 0$. The breakdown for the other four high symmetry tab configurations is very similar, with splitting taking place at large values of λ.

3.4. Parametrized tab configurations

In this section we will describe 5 tab configurations for which the locations of some or all of the tabs are determined by a single parameter, X. Again we will only present expressions for the case $r_A = r_C = ½$. It is tempting to minimize these impedance expressions in order to find optimal tab locations, but this is only useful in low symmetry configurations not presented here. For the configurations in Table 7 the optimal values X is usually evident by inspection. The reduced foil impedances for all parametrized configurations are shown in Fig. 11 where we see that the tab locations used in Table 5 are all optimal. The parametrized expressions are probably most useful when limitations of cell design or manufacturing equipment forces one to deviate from the optimal tab locations. The expressions in Table 7 can then be used to calculate the relative or absolute cost in terms of increased cell impedance caused by deviations from the optimal locations. These expressions can also be used to disentangle the effective foil impedance from stack ASI for many low symmetry tab configurations.

4. Worked examples

In this section we will present some examples of potential real world problems that can be easily solved using the results derived

Table 7
Parametrized tab configurations.

Name	Drawing	X_j {A}{C}	f_j {A}{C}	Early $\frac{R_{cell}}{R_{stack}}$	Middle $\frac{R_{cell}}{R_{stack}}$
P1	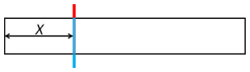	{X}{X}	{1}{1}	$\frac{\lambda\cosh(\lambda X)\cosh(\lambda\overline{X})}{\sinh\lambda}$	$1+\frac{1}{3}\lambda^2(1-3X\overline{X})$
P2		{X}{$\overline{X}$}	{1}{1}	C.2	$1+\frac{1}{3}\lambda^2(1-3X\overline{X})$
P3	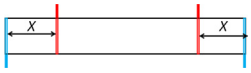	{X,$\overline{X}$}{0, 1}	$\{\frac{1}{2},\frac{1}{2}\}\{\frac{1}{2},\frac{1}{2}\}$	C.3	$1+\frac{\lambda^2}{2}\left[X(X-\frac{1}{2})+\frac{1}{6}-H^1(X-\frac{1}{2})\right]$
P4	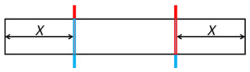	{X,$\overline{X}$}{X,$\overline{X}$}	$\{\frac{1}{2},\frac{1}{2}\}\{\frac{1}{2},\frac{1}{2}\}$	C.4	$1+\lambda^2\left[X(X-\frac{1}{2})+\frac{1}{12}-H^1(X-\frac{1}{2})\right]$
P5	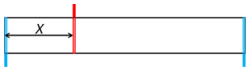	$\{\frac{1}{2}+X\}$\{0, 1}	{1}{C.5, 1 − C.5}	C.6	$1+\frac{1}{24}\lambda^2(5-12X\overline{X})$

above. Each example will be presented in the form of a question, supplemented by some required details and then the answer or solution.

4.1. I have measured the impedance of my cell. How do I subtract the effective foil impedance in order to obtain the correct stack ASI?

Details: Anode foils are 83 cm × 6.2 cm × 10 μm, cathode foils are 70 cm × 6.0 cm × 19 μm. There is a cathode tab at the core, and an anode on the outside of the jelly roll. The tabs are right next to where the active coatings start. The measured cell impedance was 30 [mΩ]

Solution: This is a very common problem which to our knowledge has not been solved in literature before. We will use the well known material properties: 1.7 [μΩ cm] and 3.1 [μΩ cm] for the Cu and Al resistivities. Based on the description, this cell has the F2 tab configuration with the anode and cathode tabs reversed, which has no effect. The steps are:

1. Calculate $R_A = \rho_A/(W_A t_A) = 1.7 \times 10^{-6}$ Ω cm/(6.2 cm × 0.001 cm) = 0.274 [mΩ cm^{-1}] and $R_C = 3.1 \times 10^{-6}$ Ω cm/(6.0 cm × 0.0019 cm) = 0.272 [mΩ cm^{-1}]. We are in luck $R_A \approx R_C$ so we need not worry about the effects of the fractional foil impedances r_A, r_C.
2. Use L = 70 cm (not 83 cm) to calculate $R_f = L(R_A + R_C)$ = 38.2 [mΩ]
3. Calculate R_{cell}/R_f = 0.785 [no units]
4. Using the coefficients for the F2 configuration in Table 6, DOD = 0 and Eq. (37) we build the equation we need to solve

$$0.785 = \frac{1}{\lambda^2} + \frac{1}{3} - \frac{1}{720}\lambda^2 + \frac{1}{30240}\lambda^4 \tag{38}$$

5. Using a numerical solver we find $\lambda^2 \approx 2.200$ [no units]. This result is much less than max λ = 10.3 so we can be confident that the expansion is accurate.

Table 8
Analytic expressions for the foil and stack heating rates.

Name	$\frac{q_{foil}}{I^2R_s}$			$\frac{q_s}{I^2R_s}$
	Early	Middle	Late	Early
F1	$\lambda\left(\frac{\frac{1}{2}\sinh 2\lambda-\lambda}{\cosh 2\lambda-1}\right)$	$\frac{1}{3}\lambda^2$	$4+4\frac{\lambda^2}{3}+q_{foil}^{early}-4\coth\lambda$	$\lambda\left(\frac{\frac{1}{2}\sinh 2\lambda+\lambda}{\cosh 2\lambda-1}\right)$
F2	$\frac{\lambda^2}{4}+\frac{\lambda}{4}\left(\frac{\sinh\lambda-\lambda}{\cosh\lambda-1}\right)$	$\frac{1}{3}\lambda^2$	$4+\frac{\lambda^2}{3}+q_{foil}^{early}-2\frac{\lambda\sinh\lambda}{\cosh\lambda-1}$	$\frac{\lambda}{4}\left(\frac{\sinh\lambda+\lambda}{\cosh\lambda-1}\right)$
F3	$\frac{\lambda}{4}\left(\frac{\sinh\lambda-\lambda}{\cosh\lambda-1}\right)$	$\frac{1}{12}\lambda^2$	$4+\frac{\lambda^2}{3}+q_{foil}^{early}-2\frac{\lambda\sinh\lambda}{\cosh\lambda-1}$	$\frac{\lambda}{4}\left(\frac{\sinh\lambda+\lambda}{\cosh\lambda-1}\right)$
F4	$\frac{\lambda^2}{16}+\frac{\lambda}{16}\left(\frac{2\sinh\frac{\lambda}{2}-\lambda}{\cosh\frac{\lambda}{2}-1}\right)$	$\frac{1}{12}\lambda^2$	$4+\frac{\lambda^2}{12}+q_{foil}^{early}-\frac{\lambda\sinh\frac{\lambda}{2}}{\cosh\frac{\lambda}{2}-1}$	$\frac{\lambda}{16}\left(\frac{2\sinh\frac{\lambda}{2}+\lambda}{\cosh\frac{\lambda}{2}-1}\right)$
F5	$\frac{\lambda}{16}\left(\frac{2\sinh\frac{\lambda}{2}-\lambda}{\cosh\frac{\lambda}{2}-1}\right)$	$\frac{1}{48}\lambda^2$	$4+\frac{\lambda^2}{12}+q_{foil}^{early}-\frac{\lambda\sinh\frac{\lambda}{2}}{\cosh\frac{\lambda}{2}-1}$	$\frac{\lambda}{16}\left(\frac{2\sinh\frac{\lambda}{2}+\lambda}{\cosh\frac{\lambda}{2}-1}\right)$
F6	$\frac{\lambda^2}{64}+\frac{\lambda}{64}\left(\frac{4\sinh\frac{\lambda}{4}-\lambda}{\cosh\frac{\lambda}{4}-1}\right)$	$\frac{1}{48}\lambda^2$	$4+\frac{\lambda^2}{48}+q_{foil}^{early}-\frac{1}{2}\frac{\lambda\sinh\frac{\lambda}{4}}{\cosh\frac{\lambda}{4}-1}$	$\frac{\lambda}{64}\left(\frac{4\sinh\frac{\lambda}{4}+\lambda}{\cosh\frac{\lambda}{4}-1}\right)$

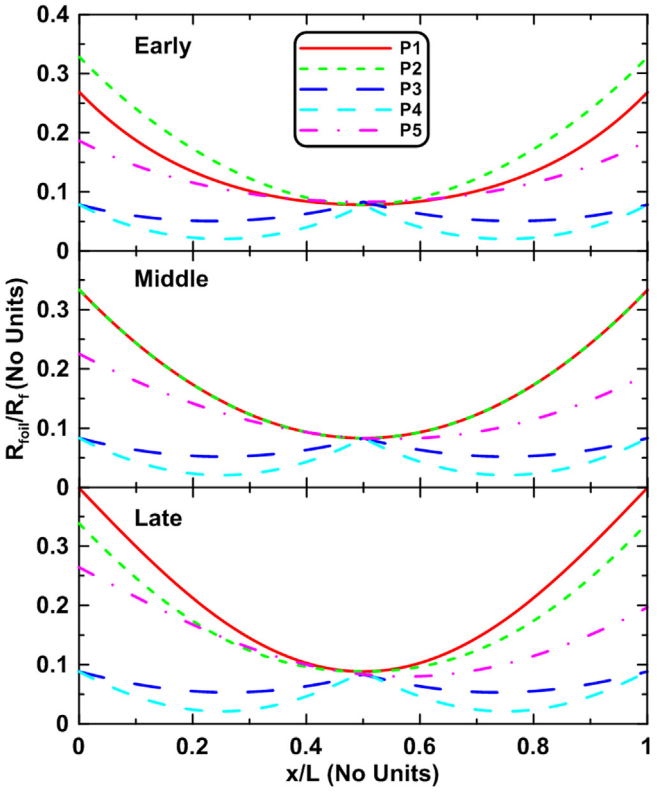

Fig. 11. Reduced foil impedance for the P1–P5 parametrized tab configurations at all three stages of discharge.

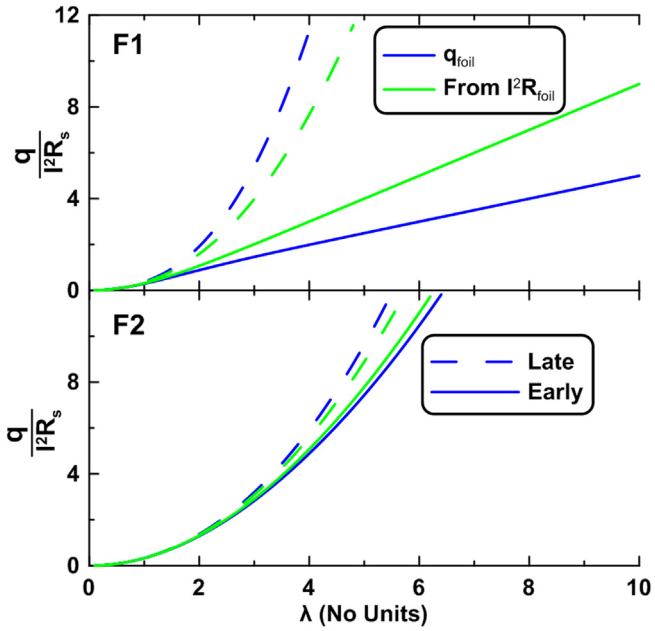

Fig. 12. Foil heating from the exact calculation and from I^2R_{foil}

6. Use Eq. (12) to find $R_s = R_f/\lambda^2 = 17.4$ [mΩ]
7. Use Eq. (12) to find the stack ASI $\rho_s = 2LWR_s = 2 \times 70$ cm $\times$ 6 cm $\times$ 0.0174[Ω] = 14.6[Ω cm^2].

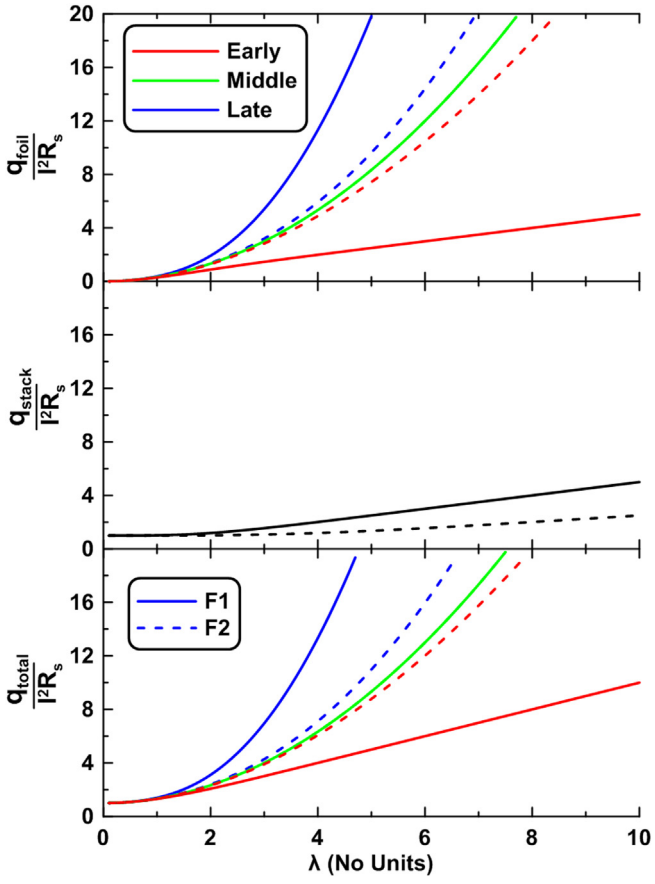

Fig. 13. Foil, stack and total heat generation rates for the F1 and F2 tab configurations.

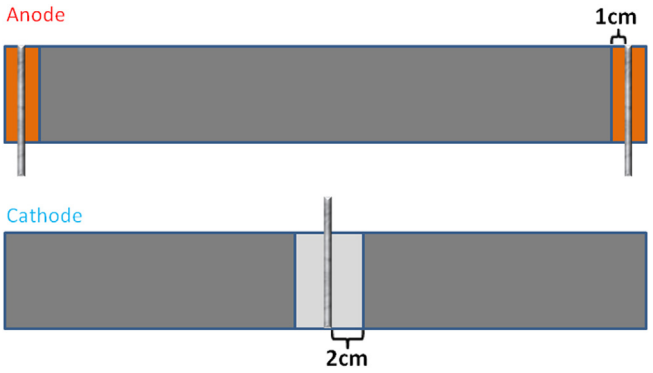

Fig. 14. Electrode design with bare foil regions near the tabs, as described in worked example #5.

If we had simply assumed that the foil impedance was negligible and used $\rho_s = 2LWR_{cell} = 25.2$ [Ω cm^2] our result would be over-estimated by about 70%! In general once you know λ everything becomes "unlocked" and you can calculate all the internal and cell level properties describe above. The foil impedance is relatively insensitive to frequency so if your measured cell impedance was from a DC pulse power test then the derived value for ρ_s will be the DC stack ASI, and correspondingly for AC.

Usually one can get good results with lower order versions of Eq. (38). For example if we ignore the last term and solve

$$0.785 = \frac{1}{\lambda^2} + \frac{1}{3} - \frac{1}{720}\lambda^2 \tag{39}$$

the result is $\lambda^2 \approx 2.199$ [no units], i.e. the difference is in the third decimal place. In fact even

$$0.785 = \frac{1}{\lambda^2} + \frac{1}{3} \tag{40}$$

gives a reasonable result $\lambda^2 \approx 2.214$ [no units]. The bottom line is that for most problems you don't need the higher order terms.

4.2. *My cell has an F3 tab configuration but I am out of luck, $R_A \neq R_C$ so I cannot use the tidy formulas in Table 5*

Solution: On the contrary, you are in luck, the formulas for the F1, F3 and F5 tab configurations just happen to be independent of the fractional foil impedances r_A, r_C so Table 5 is still valid.

4.3. *My cell has an F4 tab configuration and now I am really out of luck, $R_A \neq R_C$ so I cannot use the tidy formulas in Table 5. How do I calculate the stack ASI?*

Details: Anode foils are 83 cm $\times$ 6.2 cm $\times$ 15 μm, cathode foils are 70 cm $\times$ 6.0 cm $\times$ 15 μm. The measured cell impedance was 13 mΩ

Solution: Steps 1–3 are the same as for problem #1 above.

1. $R_A = 0.183$ mΩ cm^{-1} and $R_C = 0.344$ mΩ cm^{-1}
2. $r_A = 0.347$, $r_C = 0.653$
3. $\Delta r^2 = 0.0235$
4. $R_{Cell}/R_f = 0.352$
5. Using the coefficients for the F4 configuration in Table 6 and Eq. (B.1) we build the equation we need to solve

$$0.352 = \frac{1}{\lambda^2} + \frac{1}{12} - \frac{1}{11520}\lambda^2 + \frac{1}{1935360}\lambda^4 + 0.0235\left(-\frac{1}{192}\lambda^2 + \frac{1}{7680}\lambda^4\right)$$

6. Using a numerical solver we find $\lambda^2 \approx 3.712$.

If we had ignored the asymmetry (i.e. assume $\Delta r = 0$) we would have obtained $\lambda^2 \approx 3.718$! In general it is not easy to contrive a realistic cell design for which Δr is actually important.

4.4. How do I account for foil impedance in my cell model?

Solution:

1. Work out λ using ρ_s calculated from the stack model. ρ_s can be calculated analytically as described in the appendix of Ref. [1], or by doing a finite difference estimation $\rho_s \approx \Delta\phi_s/\Delta i_s$.
2. Choose an expression for g for your tab configuration from Table 5 and use λ to calculate a numerical value for g. For full discharges you can make g DOD dependent using Eq. (35) and follow (37).
3. Subtract $IR_f/(3g)$ from the calculated cell voltage in your model.
4. Add $I^2R_f/(3g)$ to the generated heat in your model. Use the expressions in Table 8 if you need a breakdown in terms of stack and foil contributions to the total heat.
5. Plot $I_A(X)$, $I_C(X)$, $\phi_A(X)$, $\phi_C(X)$, $\phi_s(X)$, $i_s(X)$ using (19), (20), (21), (22), (17), (2) so you can see what is going on as the simulation proceeds.

This is not the only way to use these techniques to enhance a cell model, but it is the simplest method.

4.5. My cell has bare foil segments near the tabs, your derived expressions in Tables 5 and 7 don't account for that, so guess I am out of luck?

Nope. There is no stack current and therefore no foil current divergence in the bare foil regions so you can just add the impedance of these segments to your hardware impedance.

Details: Anode foils are 180 cm × 6.2 cm × 10 μm, cathode foils are 170 cm × 6.0 cm × 19 μm. F4 tab configuration with anode and cathode tabs swapped. 1 cm bare foil on each side of the anode tabs, 2 cm bare foil on each side of cathode tab. See Fig. 14.

Solution: Any bare foil between tabs and the end of foil is irrelevant, there are no foil currents flowing there.

1. $R_A = 0.274\ \text{m}\Omega\ \text{cm}^{-1}$ and $R_C = 0.272\ \text{m}\Omega\ \text{cm}^{-1}$.
2. For the F4 tab configuration we need to worry about current splitting when calculating the effective impedance of the bare foil regions. The foil currents will be $I/2$ in all bare regions for this cell.
3. $R_H = R_{header} + R_{welds} + R_A½(1\ \text{cm} + 1\ \text{cm}) + R_C½(2\ \text{cm} + 2\ \text{cm})$
4. If you are modeling subtract IR_H from the calculated cell voltage and add I^2R_H to the generated heat in your model.
5. If you are calculating the stack ASI as in problem 1, then subtract R_H from your measured cell impedance before beginning the steps in problem 1.

4.6. I don't know how to use numerical solvers and I just want a rough estimate of the foil impedance in my cell

Solution:

- Just use the middle state geometry factors in Table 5 and then plug g into $R_{foil} = R_f/(3g)$.

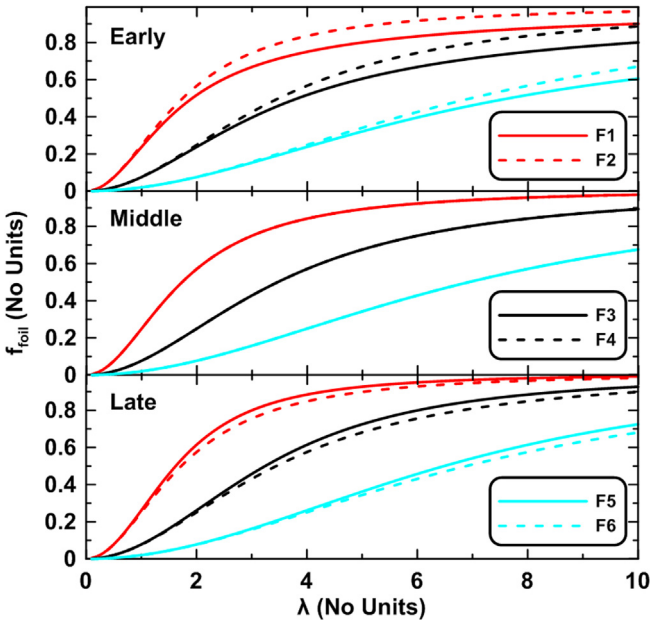

Fig. 10. Foil fraction of the cell impedance for the F1–F6 tab configurations at all three stages of discharge.

This will be very accurate for tab configurations like {F2, F4, F6} and usually "good enough" for other tab configurations. See Ref. [1] for some examples.

4.7. I want to understand the impedance of a cell with a large number of tabs, do I need to resort to numerical methods in this case because the algebra will get too complicated?

Solution: Not necessarily. For example Lee et al. [21] did large scale numerical simulations for cells with 2, 5, 10 and 20 tabs per electrode at locations $X_A = X_C = \{1/N, 3/N, 5/N \ldots N - 1/N\}$ where N is the total number of tabs. They called these configurations T2, T5, T10 and T20 respectively. Their T2 configuration is the same as the F5 configuration in Table 5. These are high symmetry configurations and as a result we can derive an expression for the reduced the cell impedance for general N

$$\frac{R_{cell}^{early}}{R_s} = \frac{\lambda}{N}\coth\frac{\lambda}{N}$$

$$\frac{R_{cell}^{middle}}{R_s} = \frac{1}{3}\left(\frac{\lambda}{N}\right)^2.$$

Nothing overly complicated about those expressions! Lee et al. calculated voltages curves which show, what looks like constant (ohmic) shifting with N. They could have got almost exactly the same result with a simple lumped foil model as described in problem 4 above.

4.8. I want to follow the steps in problem 1, but my tab configuration is not in any of the tables, now what?

Solution: If your tab configuration is not in the table then is it likely to be a low symmetry configuration with multiple tabs per electrode, which means that the fractional currents cannot be determined by symmetry or uniqueness. Here are the steps:

1. Brace yourself!
2. Convert your tab locations to dimensionless units using the active length L.
3. Use Eq. (18) to calculate expressions for $\Gamma(X_j)$ for all tab locations.
4. Calculate expressions for $\Sigma_C(X_j) - \Sigma_A(X_j)$ using Eqs. (8) and (7) with the delta functions replaced by ramp functions (see Table 1). Do this for all tab locations.
5. Calculate $\phi_A(X_j)$ for all anode tab locations. Do the same for cathode.
6. Now solve the potential matching Eqs. (23) and (24) and extract expressions for the fractional currents.
7. Choose any anode tab location X_A and any cathode tab location X_C. If the potential matching was done correctly it should make no difference which tabs you choose.
8. Calculate $r_C\Gamma(X_C) + r_A\Gamma(X_A) + r_A r_C[\Sigma(X_C) - \Sigma(X_A)]$ which will be some messy function of λ.
9. Use Eq. (26) to solve for λ as per problem 1.

We suggest you either use a computer algebra system or email the corresponding author and he will do it for you.

5. Conclusions

The analytic theory for 1D foil currents and potentials in spiral wound cells with arbitrary tab configurations has been derived. The theory has been extended to approximately account for accumulation of the gradients in the state of charge along the length of the foils. Analytic expressions for cell level properties were derived for specific tab configurations. The quality of many tab configurations was compared. We found that the common tab configurations can be categorized by their dependence on the dimensionless foil to stack impedance ratio, λ. We learned that for tab configurations with opposing anode and cathode tabs the cell impedance is strongly affected by λ and state of charge and conversely when the anode and cathode tabs are well separated the λ dependence is relatively weak. It also became clear after working a realistic numerical example that asymmetries between anode and cathode foil conductivities will have a very minor effect on the overall cell impedance, but do have some effect on the current distributions. A straight forward method is described for disentangling the foil and stack components of a measured cell impedance. The method requires one to effectively invert a non linear function of λ thereby showing why this useful process has never been obvious. The analytic theory shows us how to directly calculate the foil geometry factor introduced in a previous article [1] and we find the results are in excellent agreement with an empirically adjusted value used in numerical simulations. From the analytic results it came to light that some extra heat is generated in the stack resulting from the non-uniform stack current. It is a matter of semantics and taste as to whether or not one includes this as part of the foil heating. We also describe a simple method for adding foil effects to a stack-centric cell model. It should be clear from this article that analytic results provide a lot of insight and ease of use that numerical solutions cannot deliver. Readers should be aware this theory does not account for

1. Complex voltage curves. This will only affect the estimates of the middle and late stage cell properties.
2. Non-uniformities in the stack resistivity ρ_s. Again this is only important for the estimates of the middle and late stage cell properties.
3. Non-ohmic stack. Yet again, this is only important for the estimates of the middle and late stage cell properties
4. 2D foil effects [6]. These would be important in a very tall cell (large W) with edge joined tabs.

With these caveats in mind we would suggest that cell models can still get very accurate results using the solutions derived in this article, and not have to always resort to numerical solutions for the foil portion of the model.

The most important item on the agenda for future work is to extend this analytic theory to handle 2D systems which are relevant for flat pouch cells. Preliminary work on this problem indicates that it is also analytically tractable but very challenging.

List of symbols

For each symbol we provide example units in order to define the dimensions.

A_i	Taylor expansion coefficients for the cell impedance [no units]
DOD	depth of discharge, ranges from 0 to 1[no units]
f_{foil}	fraction of the total cell impedance caused by the effective foil impedance [no units]
f_j	fraction of the total external current flowing into tab j [no units]
g	foil impedance geometry factor [no units]
$H(X)$	Heaviside step function [no units]
$H^1(X)$	$=XH(X)$, ramp function [no units]
$i_s(x)$	current density across one layer of the stack [amp cm^{-2}]
I	total external current applied to the cell [amp]
I_A, I_C	anode and cathode foil currents [amp]
L	active length of the foils [cm]
n_A, n_C	number of anode and cathode tabs [no units]
N	$=n_A + n_C$, total number of tabs.
q	charge [Ah]
q_{cell}	total heat generation rate in the cell [watt]
q_{foil}	heat generation rate from the foil currents [watt]
q_{stack}	heat generation rate from the stack current [watt]
R_A, R_C	$=\rho_A/W_A t_A$, $\rho_C/W_C t_C$, linear anode and cathode foil resistivities [Ω cm^{-1}]
r_A, r_C	fractional foil impedances, $r_A + r_C = 1$ [no units]
Δr	deviation of r_A and r_C from ½
R_{cell}	total cell impedance [Ω]
R_{foil}	effective impedance of the foils [Ω]
R_f	$=L(R_A + R_C)$, characteristic impedance of the foils [Ω]
R_s	$=\rho_s/2LW$, total resistance of the stack [Ω]
S	convolution integration variable [no units]
t	Time [s]
t_A, t_C	thicknesses of anode and cathode foils [μm]
$V_o(x)$	open circuit voltage of the stack [volt]
V_{cell}	cell voltage, possibly under load [volt]
V_{ocv}	open circuit voltage of the cell [volt]
W_A, W_C	widths of anode and cathode foils [cm]
W	$=\min\{W_A, W_C\}$ active width [cm]
x	distance along the length of the foils [cm]
y	distance across the stack [μm]
z	distance across the width of the foils, or the height of the cell [cm]
X	$=x/L$, dimensionless distance along the length of the foils [no units]
$\overline{X}$	$=1 - X$, mirror of distance along the foils [no units]
X_A, X_C	locations of any anode or cathode tab.
∇_x	dimensioned gradient operator $\partial/\partial x$ [cm^{-1}]
∇_x	dimensionless gradient operator $\partial/\partial X$ [no units]
α^2	foil to stack impedance ratio [cm^{-2}]

$\delta(x)$	Dirac delta function.
ϕ_A, ϕ_C	anode and cathode foil potentials [volt]
$\phi_G(X, X_j)$	Greens function for unit flux at $X = X_j$ [no units]
$\phi_s(x)$	potential difference across the stack [volt]
$\phi_V(x)$	open circuit portion of the stack potential solution [volt]
$\Gamma(X)$	weighted sum of Greens functions [no units]
λ^2	$=\alpha^2 L^2$, dimensionless foil to stack impedance ratio [no units]
ρ_A, ρ_C	anode and cathode foil material resistivities [Ω cm]
ρ_s	area specific stack impedance (ASI) [Ω cm^2]
τ	time constant in the Barbashin equation of motion [s]

Superscripts:

early	early stage of a constant current discharge
middle	middle stage of a constant current discharge
late	late stage of a constant current discharge

Subscripts:

A	anode
C	cathode
j	tab index
s	stack

Appendix A. Middle state theory

When the stack current is constant: $i_s = I/2LW$ = constant Eq. (30) becomes

$$V_o(X) = \phi_s(X) + IR_s. \tag{A.1}$$

In addition Eq. (10) becomes

$$\nabla_X^2 \phi_s = IR_f[\Sigma'' - 1] \tag{A.2}$$

which can be directly solved by integration

$$\phi_s = IR_f\left[\Sigma - \frac{1}{2}X^2\right] + d. \tag{A.3}$$

The integration constant d is related to stack OCV. As mentioned above V_o represents the fully relaxed open circuit voltage across the stack long after current is turned off. If we take the average this value we get an approximation for the fully relaxed OCV of the cell. The average can be carried out using (A.1) and (A.3)

$$V_{ocv} = \int_0^1 V_o(X) = IR_f\left[\sum r_i f_i \overline{X}_j^2 - \frac{1}{6}\right] + d + IR_s$$

which can be solved for d

$$d = V_{ocv} - IR_f\left[\frac{1}{\lambda^2} + \sum r_i f_i \overline{X}_j^2 - \frac{1}{6}\right]$$

and the final expression for the stack potential is

$$\phi_s = IR_f\left[\frac{1}{\lambda^2} + \Sigma - \frac{1}{2}\sum r_j f_j \overline{X}_j^2 - \frac{1}{2}X^2 + \frac{1}{6}\right] + V_{ocv}$$

Expressions for foil currents and potentials are obtained by directly integrating (5) and (6) etc. and are shown in Table 3. We can integrate these to get

$$\begin{aligned} V_{cell} &= \phi_C(X_C) - \phi_A(X_A) \\ &= IR_f\left[r_C\Sigma_C(X_C) + r_A\Sigma_A(X_A) - \frac{r_A}{2}X_A^2 - \frac{r_C}{2}X_C^2\right] + d \end{aligned} \tag{A.4}$$

$$\begin{aligned} R_{cell} &= \frac{V_{ocv} - V_{cell}}{I} \\ &= R_f\left[\frac{1}{\lambda^2} + \sum \overline{X}_j^2 - \frac{1}{6} - r_C\Sigma_C(X_C) - r_A\Sigma_A(X_A) + \frac{r_A}{2}X_A^2 + \frac{r_C}{2}X_C^2\right] \end{aligned} \tag{A.5}$$

Appendix B. Asymmetric foil resistance

When $R_A \neq R_C$ then we cannot assume $r_A = r_C = ½$ as was done in Table 5. In this case the resulting formulas become more complicated. However we can easily extend Eq. (37) to handle the asymmetric case by setting $r_A = ½ + \Delta r$ and $r_C = ½ - \Delta r$

$$\begin{aligned} \frac{R_{cell}}{R_f} &= \frac{1}{\lambda^2} + A_0 + (1 - 2DOD)\left(A_2\lambda^2 + A_4\lambda^4\right) \\ &\quad + \Delta r^2(1 - 2DOD)\left(B_2\lambda^2 + B_4\lambda^4\right) + O\left(\lambda^6\right) \end{aligned} \tag{B.1}$$

This works for all the configurations in Table 5 except F7.

Appendix C. Long formulas

$$f_{C2} = \frac{\cosh\lambda - 1}{\cosh\lambda - 1 + \frac{\lambda}{2}\sinh\lambda} \tag{C.1}$$

$$\begin{aligned} R^{early} &= \frac{\lambda^2}{4}|2X - 1| + \frac{\lambda}{4\sinh\lambda}\left[\cosh(\lambda X) + \cosh\left(\lambda\overline{X}\right)\right]^2 \\ &\quad - \frac{\lambda}{4}\sinh(\lambda|2X - 1|) \end{aligned} \tag{C.2}$$

$$\begin{aligned} R^{early} &= \frac{\lambda^2}{16}(1 - |2X - 1|) - \frac{\lambda}{16}\left[2\sinh(\lambda X) + 2\sinh\left(\lambda\overline{X}\right)\right. \\ &\quad \left. + \sinh(\lambda|2X - 1|)\right] + \frac{\lambda}{16\sinh\lambda} \\ &\quad \times \left\{2(\cosh\lambda + 1)\left(\cosh(\lambda X) + \cosh\left(\lambda\overline{X}\right) + 1\right)\right. \\ &\quad \left. + \left[\cosh(\lambda X) + \cosh\left(\lambda\overline{X}\right)\right]^2\right\} \end{aligned} \tag{C.3}$$

$$R^{early} = \frac{\lambda}{4\sinh\lambda}\left(\cosh(\lambda X) + \cosh\left(\lambda\overline{X}\right)\right)^2 - \frac{\lambda}{4}\sinh(\lambda|2X - 1|) \tag{C.4}$$

$$f_{C1} = \frac{1}{2}\frac{(\cosh\lambda - 1)\left[2 - \cosh(\lambda X) + \cosh\left(\lambda\overline{X}\right)\right] + \sinh\lambda\left[2\lambda\overline{X} + \sinh(\lambda X) - \sinh\left(\lambda\overline{X}\right)\right]}{2(\cosh\lambda - 1) + \lambda\sinh\lambda} \tag{C.5}$$

$$R^{\text{early}} = \frac{\lambda}{8}\{[2\lambda X - \sinh(\lambda X) + \sinh(\lambda\overline{X})]f_{C1} - \sinh(\lambda X) - \sinh(\lambda\overline{X})\} + \frac{\lambda}{8\sinh\lambda}\{(\cosh\lambda + 1)[\cosh(\lambda X) + \cosh(\lambda\overline{X})] + (\cosh\lambda - 1) \times [2 + \cosh(\lambda X) - \cosh(\lambda\overline{X})]f_{C1} + 2 + 2\cosh(\lambda X)\cosh(\lambda\overline{X})\} \quad \text{(C.6)}$$

References

[1] Jan N. Reimers, J. Electrochem. Soc. 161 (2014) A118–A127.
[2] K. Amine, C.H. Chen, J. Liu, M. Hammond, A. Jansen, D. Dees, I. Bloom, G. Henriksen, D. Vissers, J. Power Sources 97–98 (2001) 684–687.
[3] Ira Bloom, Benjamin G. Potter, Christopher S. Johnson, Kevin L. Gering, Jon P. Christophersen, J. Power Sources 155 (2006) 415–419.
[4] D.P. Abrahama, D.W. Dees, J.L. Knut, I. Bloom, J.P. Christophersen, J. Power Sources 170 (2007) 465–475.
[5] Paul Nelson, Ira Bloom, Khalil Amine, Gary Henriksen, J. Power Sources 110 (2002) 437–444.
[6] J.N. Harb, R.M. LaFollette, J. Electrochem. Soc. 146 (1999) 809–818.
[7] J.N. Reimers, J. Power Sources 158 (1) (2006) 663–672.
[8] Ki Hyun Kwon, Chee Burm Shin, Tae Hyuk Kang, Chi-Su Kim, J. Power Sources 163 (2006) 151–157.
[9] Petr Krivak, Petr Baca, Milan Calabek, Karel Micka, Petr Kral, J. Power Sources 154 (2006) 518–522.
[10] Ui Seong Kim, Chee Burm Shin, Chi-Su Kim, J. Power Sources 189 (2009) 841–846.
[11] Rachel E. Gerver, Jeremy P. Meyers, J. Electrochem. Soc. 158 (7) (2011) A835–A843.
[12] Robert Spotnitz, Gowri Yeduvaka, Don Schad, Venugopal Gudimetta, Jeffrey Votteler, Gaetan Damblanc, Chris Lueth, Evan Oxenham, Steve Hartridge, Electrothermal Simulation of Spirally-wound Lithium Ion Cells, in: Abstract 1070, Honolulu PRiME, The Electrochemical Society, 2012.
[13] Meng Guo, Ralph E. White, J. Power Sources 221 (2013) 334–344.
[14] M. Doyle, J. Newman, J. Appl. Electrochem. 27 (1997) 846.
[15] Anupama Guduru, Paul W.C. Northrop, Shruti Jain, Andrew C. Crothers, T.R. Marchant, Venkat R. Subramanian, J. Appl. Electrochem. 42 (2012) 189–199.
[16] Venkatasailanathan Ramadesigan, Vijayasekaran Boovaragavan, Venkat R. Subramanian, ECS Trans. 16 (29) (2009) 129–134.
[17] Paul W.C. Northrop, Venkatasailanathan Ramadesigan, Sumitava De, Venkat R. Subramanian, J. Electrochem. Soc. 158 (12) (2011) A1461–A1477.
[18] Paul Dirac, Principles of Quantum Mechanics, fourth ed., Oxford at the Clarendon Press, 1958, ISBN 978-0-19-852011-5.
[19] E.A. Barbasin, Zaved. Mat. 1 (1957) 23–24.
[20] B.G. Pachpatte, Oxf. J. Inf. Math. Sci. 27 (2011) 99–115.
[21] Kyu-Jin Lee, Kandler Smith, Ahmad Pesaran, Gi-Heon Kim, J. Power Sources 241 (2013) 20–32.